

Growth and Characterisation of Electrodeposited Co/Cu Superlattices

Mürşide Şafak¹, Mürsel Alper^{1,*}, and Hakan Kockar²

¹Physics Department, Science and Literature Faculty, Uludağ University, Görükle, Bursa 16059, Turkey

²Physics Department, Science and Literature Faculty, Balıkesir University, Balıkesir 10100, Turkey

Ferromagnetic/non-ferromagnetic Co/Cu superlattices were grown on polycrystalline Titanium (Ti) from a single electrolyte by electrodeposition. Microstructure and magnetoresistance (MR) of the superlattices were investigated as a function of the electrolyte pH as well as the layer thicknesses. Structural characterisation by X-ray diffraction (XRD) showed that the superlattices have face-centred cubic (fcc) structure with a strong (111) texture at the studied pH levels, but the texture degree is affected by the electrolyte pH. The scanning electron microscope (SEM) studies revealed that the superlattices grown at low pH (2.0) have smoother surfaces compared to those grown at high pH (3.0). The superlattices exhibited either anisotropic magnetoresistance (AMR) or giant magnetoresistance (GMR) depending on the Cu layer thickness. The shape of MR curves changes depending on the combination of Co and Cu layer thicknesses. The superlattices with Co layers less than 3 nm and Cu layers less than 2 nm have broad and non-saturating curves, indicating the predominance of a superparamagnetic contribution, possibly due to the discontinuous nature of the ferromagnetic (Co) layer. For superlattices with the same bilayer and total thicknesses, the GMR magnitude decreased as the electrolyte pH increased. Besides possible structural differences such as the texture degree and the surface roughness, this may arise from the variation in the Cu content of the ferromagnetic layers caused by the electrolyte pH.

Keywords: Electrodeposition, Electrolyte pH, Co/Cu Superlattices, GMR.

1. INTRODUCTION

In recent years, since nanotechnology and nanoscience has been one of the new subjects attracting much attention for many researchers, the production of nanostructured materials such as superlattices, nanowires, and nanocontacts are of great importance. It has been proved that electrodeposition is a highly versatile technique to fabricate such nanomaterials.^{1–8} It also offers a number of advantages over vacuum processes such as sputtering and molecular beam epitaxy (MBE), namely, low cost, much less complex apparatus and rapid deposition at room temperature and pressure.

In particular, magnetotransport properties of ferromagnetic nanostructures such as superlattices and multilayered nanowires have been extensively studied due to potential applications ranging from magnetic field sensors to data storage devices. Most of studies have focused on Co/Cu superlattice systems because of having large giant magnetoresistance (GMR) values. The room temperature GMR magnitudes were reported 65% for sputtered

Co/Cu superlattices⁹ and 55% for electrodeposited Co/Cu superlattices.¹⁰ Of course, the GMR value of a superlattice system can vary depending on both physical parameters such as the layer thickness, bilayer number and buffer layer, and growth methods. In electrodeposition process, chemical parameters such as ion concentration in electrolytes, pH, deposition potential and additives can also influence the many properties of superlattices, in addition to the physical parameters. For example, the GMR of electrodeposited superlattices was reported to considerably affect by electrolyte composition,^{11–13} electrolyte pH,^{14–16} and additives.^{17,18} These studies demonstrated that by adjusting the chemical parameters as well as physical parameters, it could be possible to optimise and control the properties of electrodeposited superlattices, even to achieve comparable GMR values vapour-deposited ones at low magnetic saturation fields. Among the electrochemical parameters, although the electrolyte pH has a significant effect on the GMR, there are only a few studies on this topic.

The aim of the present work is to investigate the effect of the electrolyte pH on the GMR of electrodeposited Co/Cu superlattices. Therefore, a series of Co/Cu

*Author to whom correspondence should be addressed.

superlattices were grown from single electrolytes having different pH values, and their structural and magnetotransport characterisations were studied. The electrolyte pH and the layer thicknesses were observed to have a significant effect on the GMR. As the electrolyte pH decreased the GMR increased, as found in the previous work related to NiCoCu/Cu¹⁴ and NiCu/Cu¹⁵ superlattices.

2. EXPERIMENTAL DETAILS

Hexagonal close packed (hcp) Ti sheets were used as substrate. One face of each substrate was polished mechanically using emery papers of successively increasing grades and then masked with electroplating tape, except for an area of 2.9 cm² of the polished face. The uncovered area was cleaned with 10% H₂SO₄ and distilled water. After the polishing process is completed, the substrate was immersed into the electrolyte. The electrolyte used for electrodeposition of Co/Cu superlattices contained 0.75 mol dm⁻³ cobalt sulphate (CoSO₄·7H₂O), 0.02 mol dm⁻³ copper sulphate (CuSO₄·5H₂O), 0.25 mol dm⁻³ boric acid (H₃BO₃), 0.25 mol dm⁻³ sulfamic acid (NH₂SO₃H), and 0.3 mol dm⁻³ sodium sulphate (Na₂SO₄). The deposition was carried out in a three-electrode cell using an EGG Potentiostat/Galvanostat controlled by a computer potentiostatically. The counter electrode (anode) was a platinum (Pt) sheet. The reference electrode was a saturated calomel electrode (SCE). The Cu layers were deposited at a cathode potential of -0.4 V with respect to SCE while the deposition of ferromagnetic Co layers was carried out at -1.3 V versus SCE, but at this potential Cu also codeposited with Co. Therefore Cu layers contain only Cu, while the ferromagnetic layers would consist of a Co-Cu alloy. Since the Cu concentration in the electrolyte is very low, its content in the film will remain at a limited value, so the Co rich ferromagnetic layers will be mentioned as only Co layers for brevity. By switching the potential between two values used for deposition of Co and Cu layers, the superlattice films were grown according to the desired layer thickness, based on Faraday's law.

The pH value of the used electrolyte was adjusted to 2.0, 2.5, and 3.0 at room temperature by adding NaOH. Thus, the films were prepared at three different pH levels. The total thickness of all films was fixed at 5 μm, by changing the bilayer number according to the layer thicknesses of components. After growth, the films were peeled off from their substrates mechanically and mounted on glass sheets.

The crystal structure of superlattices was studied using X-ray diffraction (XRD) with Cu K_α radiation (λ = 0.15406 nm). The XRD patterns were obtained in the range of 2θ = 40°–100° with a step of Δ(2θ) = 0.02°. A scanning electron microscope (SEM) was used for morphologic observations. The film composition was determined using energy dispersive X-ray (EDX) spectroscopy in the SEM.

Magnetoresistances (MR) measurements were made at room temperature using the Van der Pauw (VDP) method with four point contacts arranged in a square (1 cm × 1 cm). The magnetic fields of up to ±8 kOe were applied parallel and perpendicular to the film plane to measure longitudinal (LMR) and transverse magnetoresistances (TMR) respectively, as described in previous work.¹⁹ In each case, the percentage change in the resistance MR(%) as a function of the applied magnetic field was calculated according to the relation $MR(\%) = \{[R(H) - R_{\min}]/R_{\min}\} \times 100$, where $R(H)$ is the value of resistance at any magnetic field H , and R_{\min} is the value at the field where the resistance is minimum.

3. RESULTS AND DISCUSSION

To determine the appropriate deposition potentials for Co and Cu layers, the electrolyte was first characterized by cyclic voltammetry (CV). The obtained CV curve is given in Figure 1. The potential scanning rate was 20 mV s⁻¹ and the size of the Ti working electrode (substrate) was the same as during the superlattice deposition. The scan was started in the cathodic direction (from 1.0 to -1.5 V vs. SCE). As seen from the Figure 1, the small peak appeared in the cathodic side at around -0.5 V corresponds to the reduction of Cu²⁺ ions. In the potential range between -0.7 and -1.0 V, a current plateau with low current is seen, indicating diffusion-limited Cu deposition. The Co deposition began at -1.0 V. Beyond this point as the potential increases, the cathodic current rises steeply due to the deposition of Co, and possibly also due to H₂

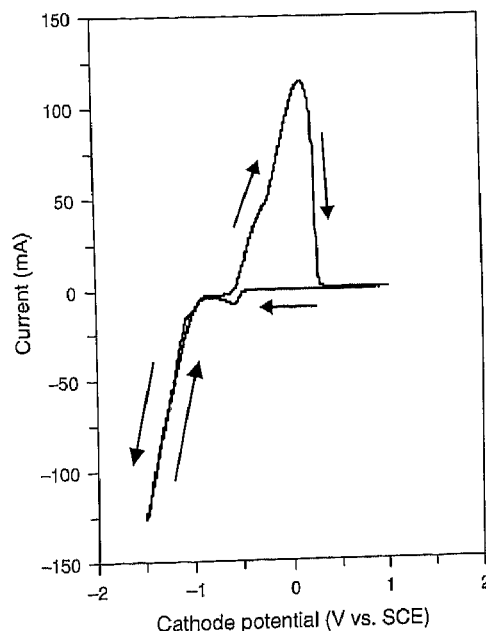


Fig. 1. Cyclic voltammetry (first cycle) of the solution used to deposit Co/Cu superlattices. The arrows show the scan direction. The scan rate is 20 mV s⁻¹.

generation. When the scan direction was reversed, the current follows the same potential dependence back to -1.0 V as in the cathodic-going scan. The broad anodic peak seen between -0.5 V and 0.4 V is due to the combination of the peaks corresponding to the dissolution of Co and Cu. The dissolution of Co and Cu was found to occur in this potential region.^{15, 16, 18, 20} Based on the CV characteristics of the electrolyte, we choose as -0.4 V for Cu deposition and -1.3 V for Co deposition.

Figures 2(a) and (b) show the current transients obtained during growth for the first few layers of two superlattices

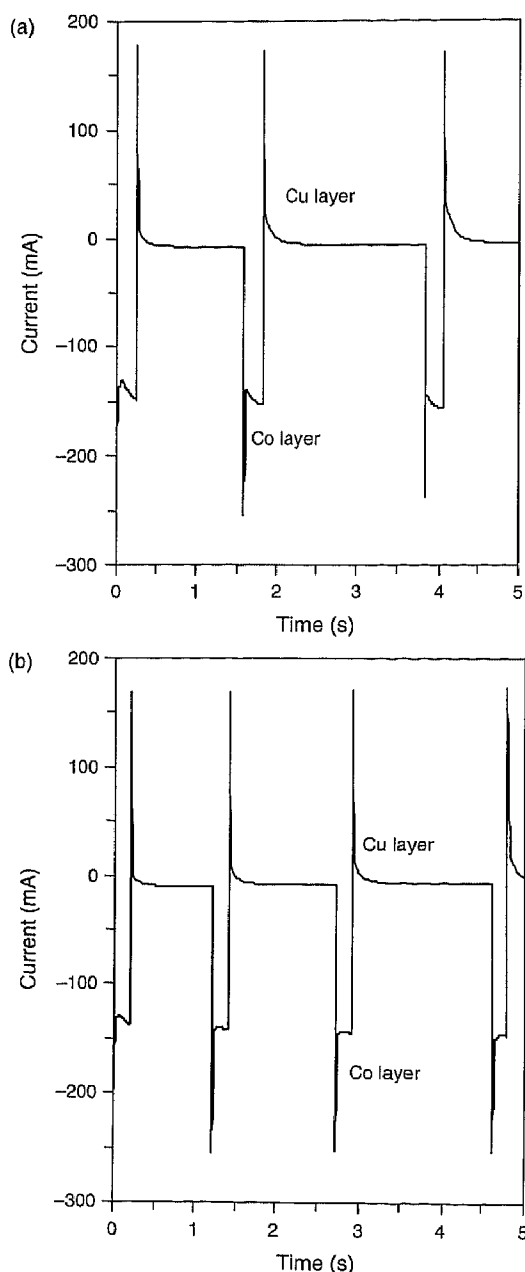


Fig. 2. Current transients for Co/Cu superlattices with the same layer thicknesses grown from an electrolyte with (a) $\text{pH} = 3.0$ and (b) $\text{pH} = 2.0$.

with the same nominal layer thicknesses but prepared at $\text{pH} = 3.0$ and 2.0 , respectively. On the cathodic (negative) side, high current pulses correspond to the deposition of Co and the low current ones to the Cu deposition. The positive current peak appeared at the beginning of each Cu deposition period is due to dissolution of Co and an exchange reaction between Cu and Co. As seen from the figure, the behaviour of the current transients for Cu deposition is the same for the superlattices prepared at each pH level, while for Co deposition they have different shapes. The current for Co deposition increases with time after an initial peak when the electrolyte pH is 3.0 , while it decreases with time for $\text{pH} 2.0$. Such a variation of the current transients with the electrolyte pH is a typical behaviour for ferromagnetic layers.^{14, 15, 20}

The crystalline structure of superlattices was studied by XRD measurements. Figure 3 shows the X-ray diffraction patterns of superlattices with $833[\text{Co}(5 \text{ nm})/\text{Cu}(1 \text{ nm})]$ nominal thickness grown from electrolytes with different pH levels. For all samples, the diffraction patterns have only characteristic peaks of a face-centred cubic (fcc) structure with a strong $\{111\}$ texture, regardless of electrolyte pH. The lattice parameters were found to be 0.3591 nm, 0.3568 nm, and 0.3549 nm for the samples prepared at $\text{pH} = 3.0$, 2.5 , and 2.0 respectively, using the least squares technique to fit experimental data to a straight line. These values are intermediate between the parameter of Cu (0.3615 nm) and that of Co (0.3544 nm), and the discrepancies in the lattice parameters are probably due to the Cu content of the films changing with the electrolyte pH.

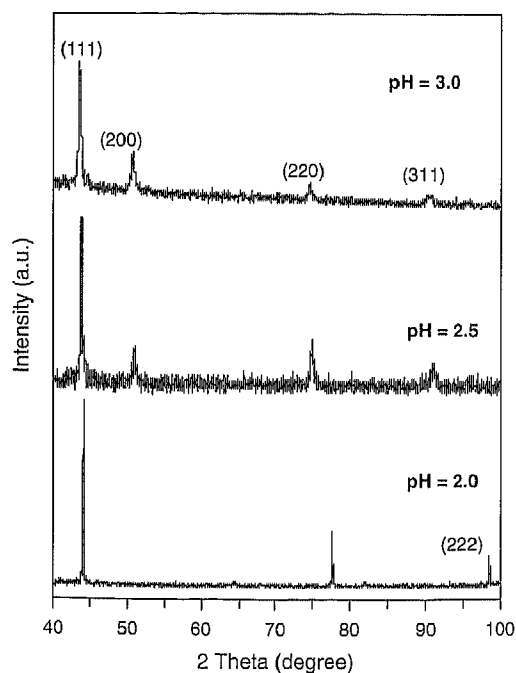


Fig. 3. XRD pattern of a superlattice with $833[\text{Co}(5 \text{ nm})/\text{Cu}(1 \text{ nm})]$ nominal thickness grown at three different pH levels. The patterns were taken after the films were removed from their substrates.

Table I. Results of the elemental analysis and MR values for Co/Cu superlattices grown at different pH levels. The negative (–) sign in MR data indicates the decrease in MR.

| pH | Samples | XRD relative integral peak intensities $I_{111}/I_{200}/I_{220}/I_{311}/I_{222}$ | EDX analysis (% atom) | | MR(%) | |
|-----|---------------------------|--|-----------------------|------|--------|--------|
| | | | Co | Cu | TMR(–) | LMR(–) |
| 3.0 | 1389[Co(3 nm)/Cu(0.6 nm)] | 100/32/21/15/NA | | | 2.0 | 0.5 |
| | 1250[Co(3 nm)/Cu(1 nm)] | | 60.3 | 39.7 | 6 | 4 |
| | 1111[Co(3 nm)/Cu(1.5 nm)] | | 52.1 | 47.9 | 4.5 | 3.8 |
| | 1000[Co(3 nm)/Cu(2 nm)] | | 44.8 | 55.2 | 3.5 | 2.5 |
| | 833[Co(5 nm)/Cu(1 nm)] | | 66.0 | 34.0 | 4.5 | 3.4 |
| 2.5 | 1250[Co(3 nm)/Cu(1 nm)] | 100/23/36/17/NA | 65.5 | 34.5 | 8.5 | 7 |
| | 833[Co(5 nm)/Cu(1 nm)] | | 69.7 | 30.3 | 10 | 7 |
| 2.0 | 1250[Co(3 nm)/Cu(1 nm)] | 100/NA/28/NA/19 | 68.2 | 31.8 | 10 | 6 |
| | 833[Co(5 nm)/Cu(1 nm)] | | 70.6 | 29.4 | 16 | 12 |

As we shall see in the EDX data below, the films contain more Cu when they are grown at high pH, so the lattice parameter of the film shifts to that of Cu. The XRD results indicate that Co had adopted the fcc structure in electrodeposited Co/Cu superlattice systems and there is a good coherency between the layers. No superlattice peaks arising from superlattice periodicity were detected, probably due to variations of the Co layer thickness caused by dissolution of Co and/or having the low quality of superlattices with total thickness as thick as 5 μm .²¹ As we shall see later, the large GMR values observed in our films confirms the superlattice structure.

The texture formation of superlattice films was evaluated by considering the relative integral peak intensities of the observed reflections. These peak intensities are listed in Table I. As can be seen, for all samples under study the (111) peak is the strongest one. As the electrolyte

pH decrease, the (200) peak weakens and at the lowest pH (2.0), (200), and (311) reflections disappear and the (222) peak occurs. This suggests that the texture formation of electrodeposited Co/Cu superlattices changes depending on the electrolyte pH.

The effect of the electrolyte pH on the surface morphology of Co/Cu superlattices was studied using SEM. Figure 4 shows the SEM images of the superlattices with 833[Co(5 nm)/Cu(1 nm)] nominal thickness deposited at (a) pH = 3.0 and (b) pH = 2.0. It is clear seen that the electrolyte pH affects the film morphology. When the superlattices were grown at low pH (2.0), they have smoother surfaces and more uniform crystallite distribution compared to those deposited at high pH (3.0).

The EDX analysis data are listed in Table I with magnetoresistance data for some samples. The data given in the EDX column of the table shows the overall composition

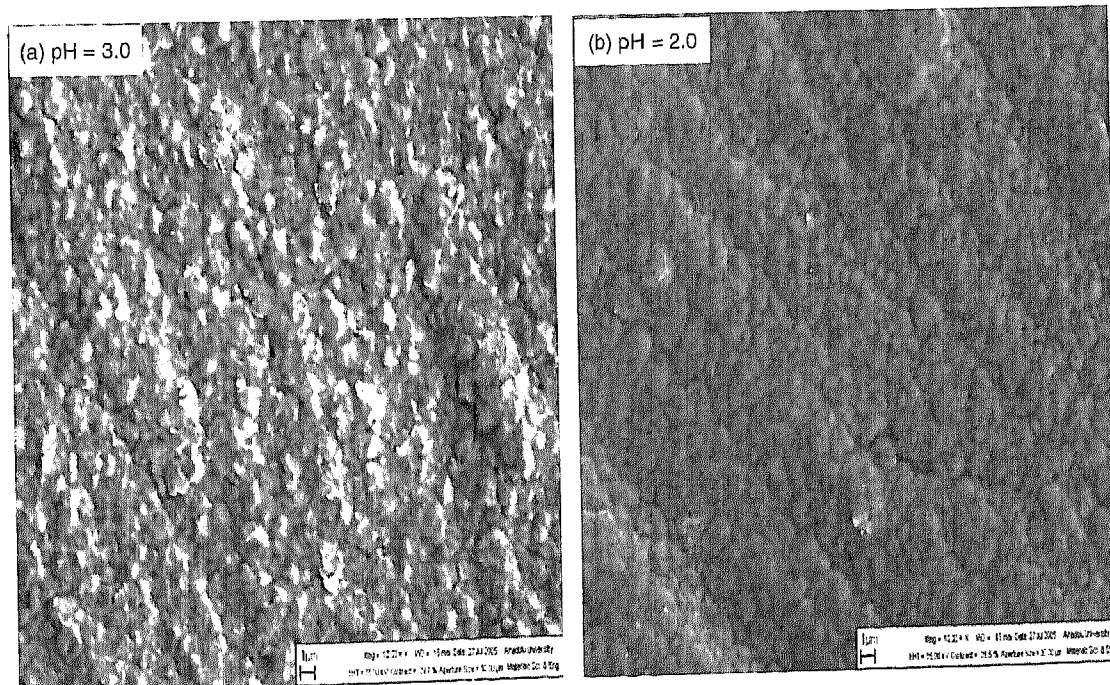


Fig. 4. SEM images of the superlattices with 833[Co(5 nm)/Cu(1 nm)] nominal thickness grown at (a) pH = 3.0 and (b) pH = 2.0.

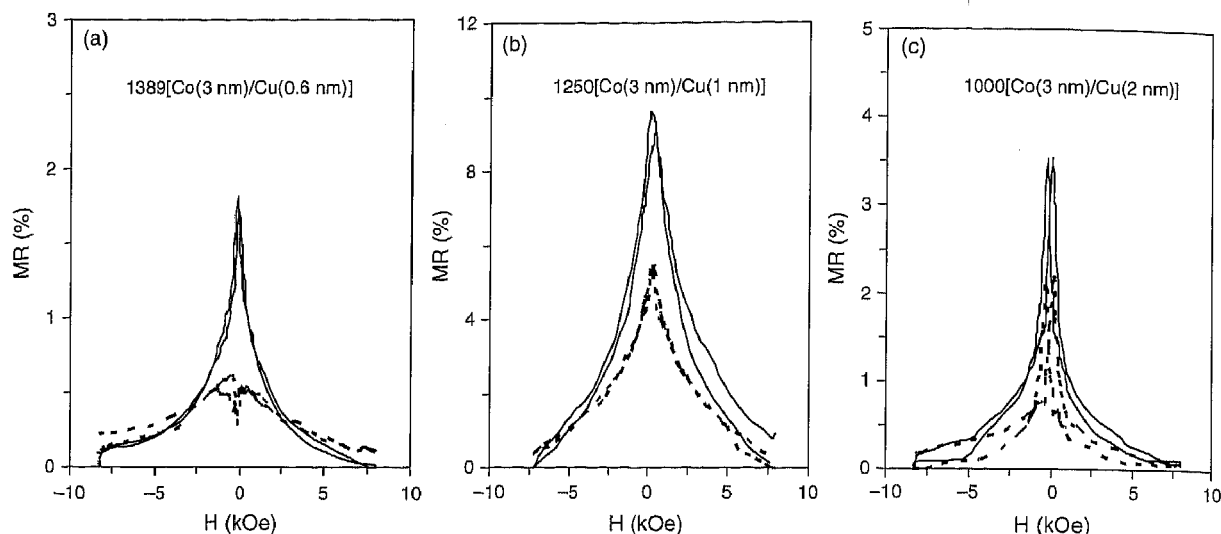


Fig. 5. Magnetoresistance curves for (a) 1389[Co(3 nm)/Cu(0.6 nm)], (b) 1250[Co(3 nm)/Cu(1 nm)], and (c) 1000[Co(3 nm)/Cu(2 nm)] superlattices. The solid line is for the transverse configuration and the dashed line is for the longitudinal configuration.

of the films grown at different pH levels. The Cu layers can be assumed to contain 100% Cu, thus the Cu content of the ferromagnetic layers can be calculated using the nominal thickness of the layers. After the Cu concentration corresponding to a Cu layer is subtracted from the overall Cu concentration, the rest is added to the ferromagnetic layer since Cu is codeposited with Co during the deposition of Co. According to this, the Cu content of ferromagnetic layers was observed to change between 10% (at.) at the lowest pH and 15% (at.) at the highest pH. The thickness of ferromagnetic layers was found to be less than the expected one. This is probably due to the dissolution of Co at the beginning of Cu deposition and also H_2 evolution during the Co deposition. On the other hand, the increase in Cu content of superlattices, and hence of the ferromagnetic layers with increasing electrolyte pH may be attributed to the different chemical reactions occurred at low and high pH.^{14, 15}

Magnetoresistance measurements were made for the superlattices with different layer thickness prepared from the electrolytes with different pH levels. The magnetoresistance of the samples with the same Co thickness (3 nm) grown at pH = 3.0 was studied as a function of the Cu thickness. For the superlattices with the Cu layer thickness less than 0.5 nm, the anisotropic magnetoresistance (AMR) effect was observed to be dominant, that is, the longitudinal magnetoresistance (LMR) increases and the transverse magnetoresistance (TMR) decreases as the magnetic field increases from zero. This may be due to the overlap of successive ferromagnetic layers with each other since the Cu layers with such very small thicknesses cannot completely separate them. The direct exchange coupling of the ferromagnetic Co layers causes a ferromagnetic alignment of the magnetisation of adjacent layers.

The superlattices with the Cu layer thickness more than 0.5 nm exhibited giant magnetoresistance (GMR). Figure 5 shows the magnetoresistance curves of superlattices with the same Co layer thickness (3 nm) but three different Cu layer thicknesses. For these superlattices, both TMR (solid line) and LMR (dashed line) decrease as the applied magnetic field increase, indicating the presence of GMR, but for the film with the Cu layer thickness of 0.6 nm there is a small field range where the AMR is dominant. Lenczowski et al. have also reported that AMR was replaced by GMR on increasing the Cu layer thickness for Co/Cu superlattices.²² As seen from Table I, the GMR magnitude reaches a maximum value for the Cu layer thickness of 1 nm, and for the superlattices with the Cu layer thicknesses larger than 1 nm, it decreases with increasing Cu layer thickness. This result is in agreement with those observed in other work on electrodeposited superlattices.^{19, 22} For the samples in this series, it is clearly seen that the magnetoresistance do not saturate in the magnetic field of ± 8 kOe. Such a behaviour of the MR was ascribed to the presence of superparamagnetic regions in the ferromagnetic layers.^{23, 24}

The Cu layer thickness was fixed at 1 nm. The magnetoresistance characteristics were studied for superlattices with two different Co layer thicknesses (3 and 5 nm) but the same Cu layer thickness (1 nm) prepared at pH levels of 2.0, 2.5, and 3.0. The MR curves of superlattices with the same nominal thickness 833[Co(5 nm)/Cu(1 nm)], but deposited at electrolyte pH values of 3.0 and 2.0 are given in Figures 6(a) and (b) respectively. If these two figures are compared, it can be seen that for both TMR and LMR components the GMR magnitudes are larger for pH = 2.0 than for pH = 3.0. The data are given in Table I with those for identical superlattices prepared at pH = 2.5. As seen from the table, as the electrolyte pH increase the

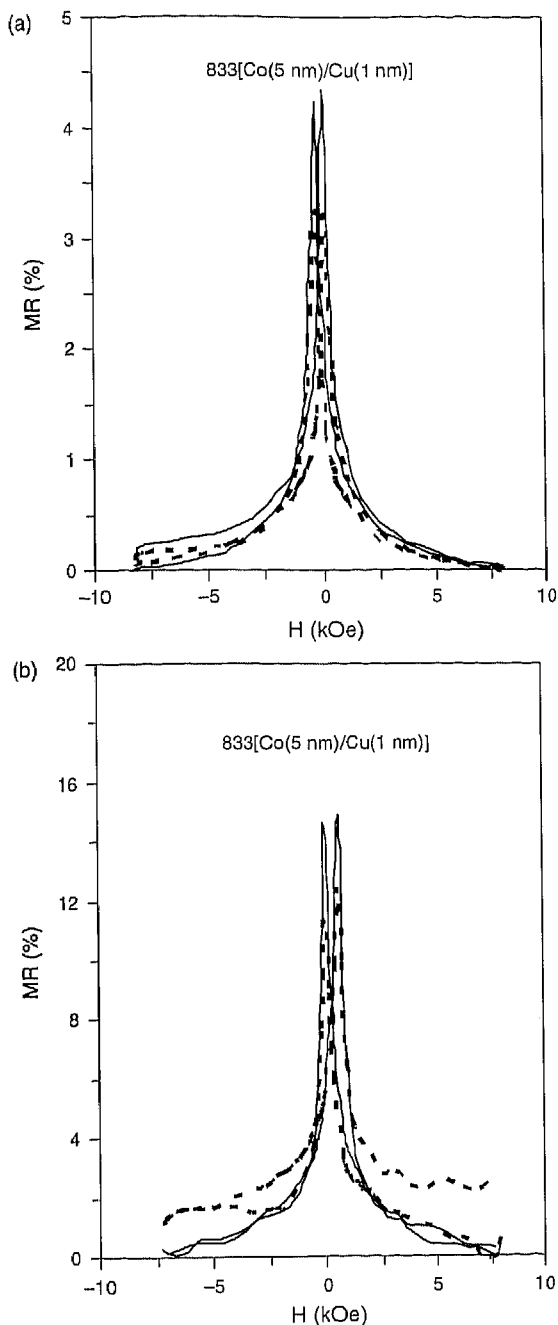


Fig. 6. Magnetoresistance curves for 833[Co(5 nm)/Cu(1 nm)] superlattices grown from the electrolytes with (a) pH = 3.0 and (b) pH = 2.0. The solid line is for the transverse configuration and the dashed line is for the longitudinal configuration.

GMR magnitude decreases. Such an effect of the electrolyte pH on the GMR magnitude was found in other electrodeposited superlattices as well.^{14–16} The effect may arise from the microstructural changes such as different texture formation and surface/interface roughness as well as different Cu contents (in ferromagnetic layers) caused by the electrolyte pH. For example, different GMR values have been reported for the samples with different crystal orientations.²⁵ Furthermore, the interface roughness caused

by the Co dissolution could be different for the films grown at low and high pH, because the amount of the Co dissolution may change depending on the electrolyte pH, the greater Co dissolution the rougher interfaces. This can give rise to ferromagnetic coupling that weakens GMR. Such a ferromagnetic coupling is expected to be stronger in the superlattices with thinner Cu layer thicknesses and for sufficiently large Cu thickness GMR is indeed observed at each pH. The fact that the interface roughness could be different for the superlattices prepared at low and high pH may also be explained by the different shapes of the Co current transients (see in Fig. 2). Further work is required to study the variation of the interface roughness with pH. Table I also shows that for all superlattices there is a difference between the LMR and TMR magnitudes, arising from the contribution of AMR to GMR, because AMR generally causes the LMR to increase and the TMR to decrease with increasing applied field.

4. SUMMARY

Co/Cu superlattices were electrodeposited on Ti substrates from electrolytes with different pH levels. The superlattices were found to have the fcc structure with a strong (111) texture, but the texture degree changes with electrolyte pH. In superlattices with the Cu layer thickness less than 0.5 nm the AMR is dominant, while the superlattices with the thicker Cu layers exhibited the GMR effect. It was also observed that the films have larger GMR values when they are prepared from the electrolyte with the low pH level (2.0). The changes in the GMR occurred depending on the electrolyte pH were attributed to microstructural such as different texture formation and surface/interface roughness and compositional effects caused by the varying pH.

Acknowledgment: This work was supported by the Scientific and Technical Research Council of Turkey (TUBITAK) under Grant no TBAG-U/74 and TBAG-1771 and Balikesir University Research Grant no 2001/02.

References and Notes

1. W. Schwarzacher and D. S. Lashmore, *IEEE Trans. Magn.* 32, 3133 (1996).
2. M. Alper, K. Attenborough, R. Hart, S. J. Lane, D. S. Lashmore, C. Younes, and W. Schwarzacher, *Appl. Phys. Lett.* 63, 2144 (1993).
3. J. Gong, W. H. Butler, and G. Zangari, *Appl. Phys. Lett.* 87, 012505 (2005).
4. J. Zhang, M. Moldovan, D. P. Young, and E. J. Podlaha, *J. Electrochem. Soc.* 152, C626 (2005).
5. P. R. Evans, G. Yi, and W. Schwarzacher, *Appl. Phys. Lett.* 76, 481 (2000).
6. G. Fasol and K. Runge, *Appl. Phys. Lett.* 70, 2467 (1997).
7. A. P. Suryavanshi and M. F. Yu, *Appl. Phys. Lett.* 88, 083103 (2006).
8. S. Boussaad and N. J. Tao, *Appl. Phys. Lett.* 80, 2398 (2002).

9. S. S. P. Parkin, Z. G. Li, and D. J. Smith, *Appl. Phys. Lett.* 58, 2710 (1991).
10. K. D. Bird and M. Schlesinger, *J. Electrochem. Soc.* 142, L65 (1995).
11. R. Coehoorn and J. P. W. B. Duchateau, *J. Magn. Magn. Mater.* 126, 390 (1993).
12. K. Megura, S. Hirano, M. Jimbo, S. Tsunashima, and S. Uchiyama, *J. Magn. Magn. Mater.* 140, 601 (1995).
13. P. Lubitz, S. F. Cheng, K. Bussmann, G. A. Prinz, J. J. Krebs, J. M. Daughton, and D. Wang, *J. Appl. Phys.* 85, 5027 (1999).
14. M. Alper, W. Schwarzacher, and S. J. Lane, *J. Electrochem. Soc.* 144, 2346 (1997).
15. M. Alper, M. C. Baykul, L. Peter, J. Toth, and I. Bakonyi, *J. Appl. Electrochem.* 34, 841 (2004).
16. V. Weihnacht, L. Peter, J. Toth, J. Padar, Zs. Kerner, C. M. Schneider, and I. Bakonyi, *J. Electrochem. Soc.* 150, C507 (2003).
17. S. Merkourakis, M. J. Hytch, E. Chassaing, M. G. Walls, and Y. L. Wang, *J. Appl. Phys.* 94, 3035 (2003).
18. L. Péter, Z. Kupay, A. Cziraki, J. Padar, J. Tóth, and I. Bakonyi, *J. Phys. Chem. B* 105, 10876 (2001).
19. M. Alper, K. Attenborough, V. Baryshev, R. Hart, D. S. Lashmore, and W. Schwarzacher, *J. Appl. Phys.* 75, 6543 (1994).
20. X. T. Tang, G. C. Wang, and M. Shima, *Appl. Phys. Lett.* 99, 033906 (2006).
21. L. Peter, A. Cziraki, L. Pogany, Z. Kupay, I. Bakonyi, M. Uhlemann, M. Herrich, B. Arnold, T. Bauer, and K. Wetzig, *J. Electrochem. Soc.* 148, C168 (2001).
22. S. K. J. Lenczowski, C. Schönenberger, M. A. M. Gijs, and W. J. M. de Jonge, *J. Magn. Magn. Mater.* 148, 455 (1995).
23. I. Bakonyi, J. Toth, L. F. Kiss, E. Toth-Kadar, L. Peter, and A. Dinia, *J. Magn. Magn. Mater.* 269, 156 (2004).
24. M. Shima, L. Salamanca-Riba, R. D. McMichael, and T. P. Moffat, *J. Electrochem. Soc.* 148, C439 (2002).
25. G. Nabiyouni and W. Schwarzacher, *J. Magn. Magn. Mater.* 156, 355 (1996).

Received: 20 June 2006. Revised/Accepted: 11 February 2007.